

KI-PMF: Knowledge Integrated Plausible Motion Forecasting

Abhishek Vivekanandan¹, Ahmed Abouelazm¹, Philip Schörner¹, J. Marius Zöllner^{1,2}

Abstract—Accurately forecasting the motion of traffic actors is crucial for the deployment of autonomous vehicles at a large scale. Current trajectory forecasting approaches primarily concentrate on optimizing a loss function with a specific metric, which can result in predictions that do not adhere to physical laws or violate external constraints. Our objective is to incorporate explicit knowledge priors that allow a network to forecast future trajectories in compliance with both the kinematic constraints of a vehicle and the geometry of the driving environment. To achieve this, we introduce a non-parametric pruning layer and attention layers to integrate the defined knowledge priors. Our proposed method is designed to ensure reachability guarantees for traffic actors in both complex and dynamic situations. By conditioning the network to follow physical laws, we can obtain accurate and safe predictions, essential for maintaining autonomous vehicles’ safety and efficiency in real-world settings. In summary, this paper presents concepts that prevent off-road predictions for safe and reliable motion forecasting by incorporating knowledge priors into the training process.

Index Terms—Safety, Motion Forecasting and Planning, Knowledge Integration

I. INTRODUCTION

In complex driving scenarios, accurate and reliable short-term trajectory predictions of surrounding actors are essential for maintaining safe and efficient driving performance. For such traffic actors, their intention is often multi-modal and exhibits plausibility in their action space. For modeling such a prediction space, through Deep Neural Networks, this multi-modality often encompasses uncertainty leading to implausible future states. In the case of applications where safety is critical, this can lead to fatal situations due to the network’s inability to learn from prior knowledge, as shown in [1, 2]. The limitations mentioned above pose significant challenges to the implementation of these approaches in autonomous driving systems aimed at ensuring safety.

In this work, we propose a novel multi-stage architecture for integrating explicit knowledge (we use the term *constraints* interchangeably to represent *priors* throughout this work) into a learning-based trajectory forecasting model to ensure plausible motion forecasts for the traffic participants. Our network comprises two stages. The first stage is a deterministic, non-parametric refinement layer that uses explicit environmental and kinematic constraints to compute plausible trajectories. We represent the problem of multi-modal trajectory prediction as a classification problem by constructing the future reachable states as a set of trajectories

¹ FZI Research Center for Information Technology, 76131 Karlsruhe, Germany. {vivekana, abouelazm, schoerner, zoellner}@fzi.de

² Karlsruhe Institute of Technology (KIT), Germany.

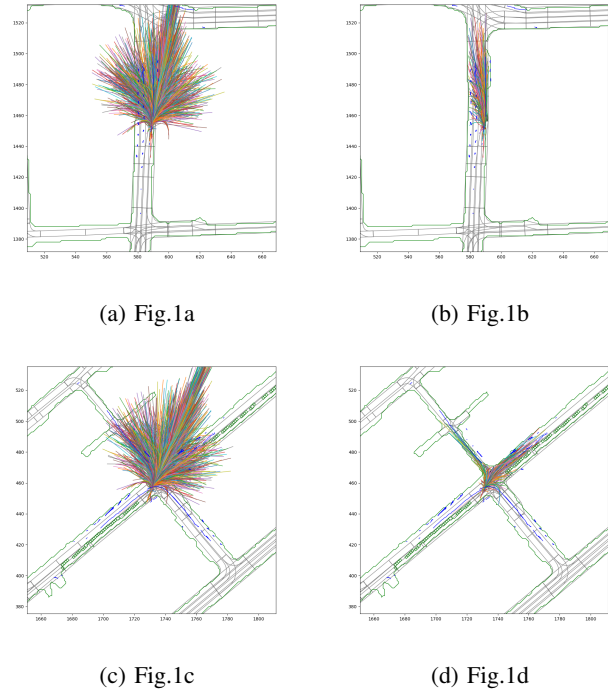


Fig. 1: The left column represents the two scenes with unrefined trajectories injected into the scene. The right column represents the impact of our refinement layer, where we refine the original trajectory set with priors, allowing us to avoid predicting in the off-road areas.

following the works by Phan-Minh et al. [3]. This method of output representation allows us to encode non-holonomic vehicle constraints into the model, which otherwise would be difficult. Environmental constraints, derived from HD maps M , are encoded as polygons to perform a Point-in-Polygon search. This process further refines the trajectories, preventing any off-road predictions. The advantage of such a non-parametric search is ensuring that the proposals are interpretable. The second stage utilizes these refined proposals and combines them with goal positions [4] to learn a plausible representation space. This method of fusing lanes and trajectories allows the network to learn reachability-based features from a scene at a global level for the target actor.

The main contributions of this work are as follows:

- Two staged approach of trajectory generation and prediction with constraint-based refinement layer which provides feasibility and safety assurance to exclude off-road trajectories and thereby implausible states.

- Multi-headed attention layers, which focus on learning from interactions between feasible trajectories and corresponding goal-based reachable lanes.
- Extensive runtime analysis to showcase the real-time capabilities of the refinement layer.

II. RELATED WORK

Scene representation and encoding is a functionally important part of the motion forecasting stack, where the representation is learned from rasterized inputs through the use of CNNs to extract features as seen in ChauffeurNet [5]. A sensor-independent feature representation in a spatially discretized grid is proposed in [6], where a 2D CNN encoder-decoder architecture is used to predict the environment. Stacking of rasterized images is inducted into the multi-modal prediction architecture through the works from [7] where different heads are used for regressing trajectories as waypoints and classification heads for estimating the softmax probabilities of the trajectories.

Rasterization was quickly replaced by vector-based methods such as VectorNet [8] and LaneGCN [9] due to the prohibitively high compute cost and limitations arising from the receptive field of CNNs.

Generalization Limitations, the limited generalization and lack of safety guarantees in trajectory forecasting networks were investigated in [1], where adversarial scenarios are generated to showcase the off-road predictions of the networks. State-of-the-art methods such as WIMP [10] and LaneGCN had higher off-road or physically infeasible trajectories, making them not generalizable. This empirical evidence prompted us to pivot towards the explicit incorporation of prior knowledge, with the aim of attaining safety guarantees in predicted trajectories. Although prior knowledge integration and plausibility-based checks are done for applications related to 3D object detectors [11], our work is the first to extend it to motion forecasting problems.

Vehicular motion constraints for motion forecasting problems have been studied through the works of [12–14], where a combination of machine learning-based approach is overlaid on top of an optimizer to solve for assurance. While these methods ensure the generation of safe trajectories, they do not incorporate feasibility guarantees within the learning process but rather as a post-processing step, which can result in unnecessary computational resource consumption. The problem of motion forecasting was typically dominated by regression-based methods such as learning constraints via a kinematic layer through vehicle dynamics modelling from [15, 16]. While they prevented the infeasible trajectories based off on turn-rate, they had no upper bounds to guarantee the off-road predictions from the lack of environmental constraints. Similarly, Covernet [3] captured the vehicle dynamics into a set of trajectories to represent the future motion of the actors. They then trained a network to pick the best trajectory for the observation from the set of trajectories, making the problem space a classification task. Some limitations of the discussed approach include the absence of feasibility guarantees for the generated trajectories, as certain

trajectories are derived from dataset samples, and the reliance on rasterized inputs, which constrains their applicability in online methods. Although PRIME [17] addresses the integration of learning and trajectory generation within a single pipeline, it generates trajectories in Frenet space by varying the terminal lateral distance and velocity of a Frenet trajectory. This transformation of each actor into a separate Frenet space, which may lead to challenges in handling interactions among multiple actors.

In this work, we propose a novel approach that prevents off-road predictions and guarantees physically valid trajectories through the usage of a non-parametric refinement layer. The guarantees are derived by including physical and outer constraints into the trajectory generation and consequently propagated into the learning components of the network for reliable predictions.

III. METHODOLOGY

A. Problem formulation

The objective of motion forecasting in autonomous driving deals with predicting the future possible motions of actors in a given scenario. The estimated tracks of surrounding actors are assumed to be given through an existing perception system. Given a target actor a_{tar} for prediction, trajectory forecasting utilizes not only the past observed trajectories of a_{tar} but also of other actors in its vicinity a_{other} over a finite time window t_p for accurate prediction of its future trajectory over a prediction horizon t_h . A past trajectory $T_{p,i}$ of an actor a_i is represented by a sequence of states, as shown in equation 1, where s_i^t represents the centerpoint location (x, y) of the actor i at a time t in a Cartesian coordinate frame. The set of all actors' past trajectories is noted as Γ_p .

$$T_{p,i} = \{s_i^{-t_p}, s_i^{-t_p+1}, s_i^{-t_p+2}, \dots, s_i^0\} \quad (1)$$

Similarly, the future predicted trajectory $T_{h,i}$ of a target actor a_i is a sequence of predicted center point coordinates, as seen in equation 2. Such that the set of all actors' future trajectories is Γ_h .

$$T_{h,i} = \{s_i^1, s_i^2, s_i^3, \dots, s_i^{t_h}\} \quad (2)$$

Moreover, we utilize HD map information, as illustrated in Figure 2, where each lane within a query window is discretized and encoded as a set of centerline (x, y) points in a coordinate system relative to the prediction target agent a_{tar} . The components involved in the architecture will be discussed in more detail in the following sections. By incorporating HD map information, the model can better understand the surrounding environment and enhance the accuracy of trajectory predictions

B. Integration of Domain knowledge: First Stage

The first stage takes the trajectory sets as input along with lane centerlines (converted to a vector representation from HD map) to produce feasible trajectories that respect the constraint conditions. To generate an initial set of trajectories, we rely on a similar bagging algorithm like Covernet [3]

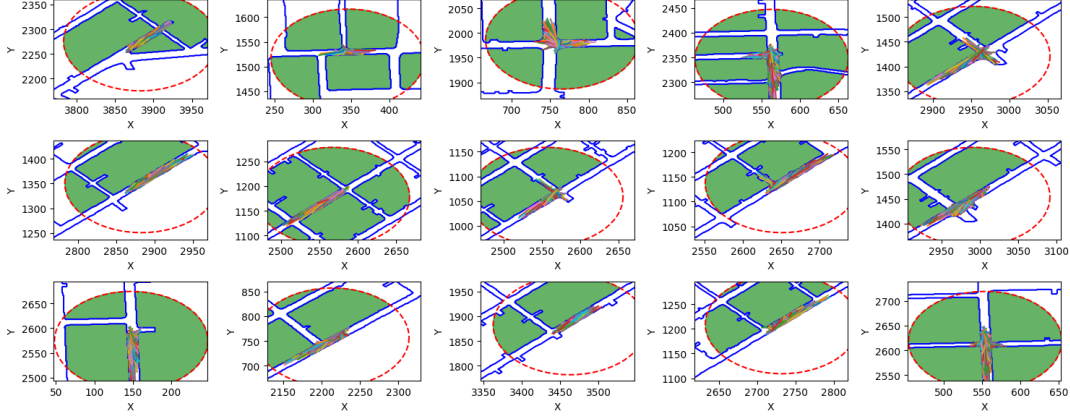


Fig. 2: The green region defines the local buffer polygon, which is used to reduce the size of the main polygon area. The blue linear lines represent the polygons. Here we use a circular buffer (red dotted circle) for concept explanation. The exteriors of the green polygons are then checked for collisions to make the computation of the trajectory-in-polygon faster. The x and y-axis are represented in the city coordinates system.

on Argoverse dataset [18] with coverage $\epsilon \simeq 2m$, where coverage is the maximum distance between two neighboring trajectories in the set. The resulting trajectory set Γ_{set} is considered to be dynamic. Although the algorithm is good enough to find a diverse set of trajectories, we still apply kinematic constraints to fit the curvature assumptions of a trajectory. This results in a set that guarantees the properties of being smooth and kinematically feasible.

Coordinate transformation The motion of target actors and HD map are represented in a city coordinate system [18] whereas the trajectory sets are in Cartesian coordinates. To define a common relative representation for the networks to learn from, we use the curvilinear-based relative coordinate system to project the actors' motions and trajectories, as can be seen from lines 1 – 8 in algorithm 1.

The Refinement Layer takes in a trajectory set $\Gamma_{set} = \{T_0, T_1, \dots, T_{n-1}\}$ and prunes them based on a trajectory's plausibility of existence derived from the HD map. Using prior knowledge about the lane widths from the Lane centerlines, we can delineate the boundary regions, allowing us to regress the drivable regions. This construction results in boundary envelope polygons (blue lines, as can be seen from Fig. 2) surrounding the outermost centerline, which can then be used to generate upper and lower sampling bounds for trajectories. A trajectory T_i is plausible and considered valid if and only if $\forall(x, y) \in T_i, (x, y) \in Polygon_b$. A detailed representation of the refinement layer workings can be seen from the following algorithm 1.

Goal lanes are target lane approximations that guide the networks to learn “where to go” information within the scene. The “which” information is provided by picking the best trajectory to fit the “where” embeddings. We use a simple beam search on the lane centerlines with a radius of $100m$ w.r.t heading angle of the target actor. This results in possible $Goal_{lanes}$, which are then passed on to the Lane Encoder part of the network for extracting features.

Algorithm 1 Refinement Layer

Require: Trajectory set Γ_{set} , HD-map M
Ensure: Feasible trajectories $\Gamma_f \leftarrow$ Local coordinate system

- 1: $origin \leftarrow$ Query origin of the target actor a_{tar}
- 2: $tangent \leftarrow$ Query tangent vector of the nearest lane l to a_{tar}
- 3: $\theta \leftarrow$ Calculate rotation angle from the tangent vector $tangent$
- 4: $R \leftarrow$ Rotation matrix with rotation angle θ
- 5: **for** each actor i in scene **do**
- 6: Calculate displacement offsets dx, dy for waypoints defining the trajectories
- 7: $\hat{dx}, \hat{dy} \leftarrow (dx, dy) \cdot R$ {Rotation into curvilinear coordinates}
- 8: **end for**
- 9: $Goal_{lanes} \leftarrow$ Query centerline points of nearby lanes to find reachable goal positions.
- 10: $Polygon_b \leftarrow$ Construct buffer polygon boundaries from a given lane width from a given lane centerline {In the city coordinate system}
- 11: $\Gamma_{set} \leftarrow \Gamma_{set} \cdot R$
- 12: **for** each trajectory $T_i \in \Gamma_{set}$ **do**
- 13: **for** each polygon envelope in $Polygon_b$ **do**
- 14: **if** $T_i \cap Polygon_b \neq \emptyset$ **then**
- 15: $\Gamma_{set} \setminus T_i$
- 16: **else**
- 17: Continue
- 18: **end if**
- 19: **end for**
- 20: **end for**
- 21: $\Gamma_f \leftarrow \Gamma_{set} \cdot R$ {Rotation to local coordinate system}
- 22: **return** $\Gamma_f, Goal_{lanes}$

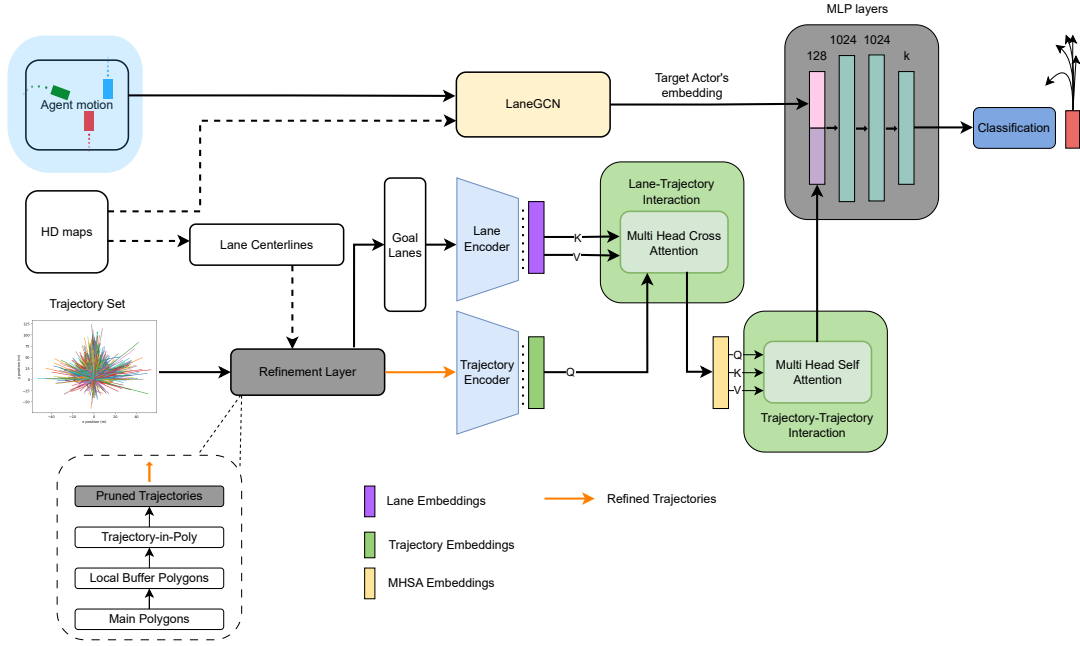


Fig. 3: High-level overview of the architecture. The Refinement layer takes two inputs. 1. Lane centerline points in the map coordinate system for a given query window (in meters) and 2. trajectory sets from Covernet with $\epsilon = 2$ coverage. The refinement layer produces feasible/pruned trajectories by constructing a lane boundary given the lane-centerline points. It also produces a list of possible goal positions or reachable lanes where the target actor could reach for within a given prediction horizon. LaneGCN is used as a backbone architecture and outputs an embedding representation for a_{tar} which is then concatenated with the lower parts of the network.

C. Encoder

Given the $Goal_{lanes}$ and feasible trajectories generated by the refinement layer, we propose learned layers to consume the information and project it into a high-dimensional vector space. Furthermore, we propose the utilization of attention layers to learn interactions between trajectories and lanes. Finally, the encoded feature vector of the trajectories can be extended by the target actor features to enrich its information before passing the final trajectories' representation to a classification head, as shown in Fig. 3.

1) *Learning Goal lanes representation:* $Goal_{lanes}$ is a set of lanes, generated by the refinement layer, that the target actor can traverse given its current heading direction. A goal lane $L_i \in Goal_{lanes}$ is an ordered set of centerline points on the lane given the direction of the actor's motion, such that $L_i \in \mathbb{R}^{n_i \times 2}$. Each scene can have several goal lanes R , and each lane L_i can have a different number of centerline points n_i as a result of differences in road topology and reachabilities. Thus, the goal lanes are dynamically padded during pre-processing such that all lanes in the same scene have the same length N . Furthermore, each goal lane is extended with an additional flag set to zero for locations in the lane that are padded. Accordingly, the goal lanes are represented as a set $Goal_{lanes} \in \mathbb{R}^{R \times N \times 3}$. The Lane Encoder utilizes temporal convolution and bidirectional LSTM to learn representations of the input $Goal_{lanes}$.

2) *Learning feasible trajectories' representation:* A feasible trajectory is a reachable state for the a_{tar} , adhering to

the road topology and the physical constraints of a vehicle model. The Trajectory Encoder is designed to consume the set of feasible trajectories, $\Gamma_f \in \mathbb{R}^{D \times t_h \times 2}$, to learn a high-dimensional representation of each trajectory independently using a temporal convolution and an LSTM.

D. Attention Layer

In order to model the interactions between $Goal_{lanes}$ and feasible trajectories Γ_f for, a_{tar} we employ the attention mechanism as described in [19]. Multi-Head Cross-Attention layer enables the mixing of two different input sequences, allowing for a more comprehensive understanding of the relationship between the actor's probable heading (choose the best lanes) and the best state to execute (choose the best trajectory). Thus, our Lane-Trajectory interaction block takes the trajectory and lane embeddings to perform cross-attention. This is achieved by linear projection of trajectory embeddings as queries (Q), and lane embeddings as keys (K) and values (V) in the QKV formulation. The output embeddings from this block are then passed onto the next Trajectory-Trajectory interaction block based on self-attention. Multi-Head Self-attention (MHSA) provides the network with an intuitive understanding of global trajectories, facilitating local routing of information amongst each other. In other words, the MHSA layer allows trajectories to communicate with each other, enhancing the overall understanding of the relationships between trajectories in the set. For computational efficiency, we use multi-head attention

in both these blocks with eight heads.

$$\text{Attention}(Q, K, V) = \text{softmax}\left(\frac{QK^T}{\sqrt{d_k}}\right)V, \quad (3)$$

1) *Representations fusion and network output*: The feature representation of a_{tar} , obtained from the A2A layer of the LaneGCN, is combined with the feasible trajectories' representation from the Trajectory-Trajectory interaction block. This combination informs the trajectories of interactions between a_{tar} and a_{others} in the scene. The concatenated representation is then fused using an MLP layer. Finally, the trajectories' representation is passed through the classification head to learn the probability of each trajectory. The classification head is a sequential module of a linear residual block [20] that maintains the input dimensionality, followed by a linear layer that modifies the output dimensionality to be equal in size to the number of feasible trajectories. Thus, the network output P is a vector with the same size as the number of feasible trajectories in the scene, such that $P \in \mathbb{R}^D$. Each element in the vector provides an estimate of the occurrence probability of the corresponding trajectory.

E. Loss Learning and Trajectory Scoring

The classification loss of the network is based on the loss function proposed in [17, 21]. The proposed loss calculates the cross-entropy loss based on the distance between the feasible trajectories and the ground truth trajectories compared to the probabilities estimated by the network. The loss calculation requires the set of feasible trajectories $\Gamma_f \in \mathbb{R}^{D \times 30 \times 2}$, the target actor ground truth trajectory $\Gamma_G \in \mathbb{R}^{1 \times 30 \times 2}$, assuming a prediction horizon $t_h = 30$, and the network output $P \in \mathbb{R}^D$ over the feasible trajectories. This loss function motivates the network to assign higher probabilities to feasible trajectories with a small distance to the ground truth trajectory. These probabilities are calculated based on the Euclidean distance between the ground truth trajectory and the feasible trajectories generated by the refinement layer. Equation 4 illustrates the calculation of the target probability for the i^{th} feasible trajectory $T_{f,i}$, where τ is a hyperparameter denoted as temperature factor

$$\psi(T_{f,i}, \Gamma_G) = \frac{\exp(-\text{Dist}(T_{f,i}, \Gamma_G)/\tau)}{\sum_{j=1}^k \exp(-\text{Dist}(T_{f,j}, \Gamma_G)/\tau)}. \quad (4)$$

$\text{Dist}(\cdot)$ is a metric distance that calculates the maximum distance between two trajectories based on the L2 difference of their (x, y) coordinates per time step, as demonstrated in equation 5. The predicted network probabilities $\gamma(\Gamma_f)$ are calculated by applying softmax activation on the network output P . Finally, the classification loss is calculated as the cross-entropy loss between predicted probabilities $\gamma(\Gamma_f)$ and the target probabilities $\psi(\Gamma_f, \Gamma_G)$.

Trajectory selection Additionally, top-k selection of feasible trajectories is applied in the loss calculation to avoid exhaustive backpropagation of the loss over all the feasible trajectories. In the loss calculation, the top-k trajectories are the k_{top} trajectories with the highest ground truth probabilities, requiring the network to learn a better classification

performance over the most similar trajectories to the ground truth. It should be clarified that in the network evaluation phase, the top-k trajectories for computing the evaluation metrics are computed based on the top-k predicted probabilities by the network and have no access to the ground truth information at all. Thus, avoiding injecting any bias or ground truth information into the evaluation process.

$$\text{Dist}(T_{f,i}, T_{f,j}) = \max\left(\left\|s_1^i - s_1^j\right\|_2^2, \dots, \left\|s_{t_h}^i - s_{t_h}^j\right\|_2^2\right) \quad (5)$$

IV. EXPERIMENTS

A. Dataset

We use the Argoverse-1 motion forecasting dataset [18] which comprises 205942 scenes for training, 39472 for validation. Every scene consists of a target actor whose past motion is fully observable throughout the scene. A scene also encompasses other actors, whose motions can be partially or fully observed. For a_{other} which have missing observations, we apply zero padding to fully match the shape of the target actor. The training and validation epochs are run with the aim of predicting the target actor's future reachable state given the past observations of itself along with other actors in the scene. The observation horizon is $2s$ and the prediction horizon is $3s$, both of them sampled at $10Hz$.

B. Covernet trajectories

We use the Covernet trajectory set having a $\epsilon = 2$ with 2800 trajectories. Although Covernet has a trajectory set with, $\epsilon = 3, 8$ we chose to use, $\epsilon = 2$ as it has dense coverage enough to justify the capabilities of our approach. The trajectories are upsampled and translated to fit the local coordinate system. We also calculate the lower bound achievable with the calculated trajectory sets, as can be seen from Table I, through minADE calculation between the ground truth trajectory and the closest trajectory from the set. This is the theoretical lower limit achievable by training.

C. Metrics

We evaluate our approach using standard metrics employed in prior studies, namely the minimum Average Displacement Error (minADE), minimum Final Displacement Error (minFDE), and Miss Rate (MR) for both single-modal ($k = 1$) and multi-modal ($k = 6$) predictions. Along with these standard metrics, we provide evaluations for drivable area compliance (DAC) [18]. For a model that produces a trajectories out of which b trajectories violate road boundary constraints, the DAC for the model results in $(a - b)/a$. A higher DAC indicates higher compliance with the drivable area. The minADE metric measures the minimum average Euclidean error between the predicted trajectory and the ground-truth trajectory of the target vehicle. Similarly, minFDE measures the minimum Euclidean error between the predicted endpoint and the ground-truth endpoint. The ratio of sequences in which none of the predicted endpoints exceeds 2 meters from the ground-truth endpoint is called the MR.

TABLE I: Quantitative comparison of different metrics on argoverse validation split

Models	LowerBound		K=1			K=6			DAC
	minADE	minFDE	minADE	minFDE	MR	minADE	minFDE	MR	
Argo-NN+Map (prune)	Reg	Reg	3.38	7.62	0.86	1.68	3.19	0.52	0.94
Argo-NN	Reg	Reg	3.45	7.88	0.87	1.71	3.29	0.54	0.87
Argo-CV	Reg	Reg	3.53	7.89	0.83	-	-	-	0.88
WIMP [10]	Reg	Reg	1.43	6.37	-	1.07	1.61	0.23	-
LaneGCN [9]	Reg	Reg	1.71	3.78	0.67	0.90	1.77	0.26	-
Covernet $\epsilon = 2$ [3]	1.02	0.68	3.46	8.70	0.78	1.85	3.83	0.44	-
LaneGCN (Pre-trained)+Ours	1.02	0.68	1.97	4.72	0.73	1.55	2.04	0.25	0.99
LaneGCN (Full)+Ours	1.02	0.68	1.82	4.23	0.69	1.52	1.94	0.22	0.99

D. Training details

The complete network is trained for 38 epochs with Adam optimizer [22] on a NVIDIA A100 GPU. The optimizer has a learning rate of 10^{-3} for the first 30 epochs and changes to 10^{-4} for the next 8 epochs; with a batch size of 32. All layers in the architecture have a dimension of 128. The number of heads in the attention layer is 8. The temperature factor τ and k_{top} are set to 1 and 6 in the loss calculation.

E. Computational performance

Although the refinement layer does not have any learnable parameters, it requires computation time to perform the refinement, which is crucial for the real-time deployment of the network. In our refinement layer we use the trajectory-intersects-polygon operation (similar to point-in-polygon), on average per scene, we were able to perform a check in $0.3 - 0.5ms$ for 4 polygon envelopes on 12 core CPU. The intersection test could be parallelized easily, allowing for a significantly faster computation on a GPU. On average, there were 948 trajectories available after the refinement layer, with four goal positions constructed per a_{tar} per scene. The Fig. 4 showcases the theoretical limits for a point-in-polygon operation, which we performed using different algorithms on a CPU for a total of 1 million randomly sampled points.

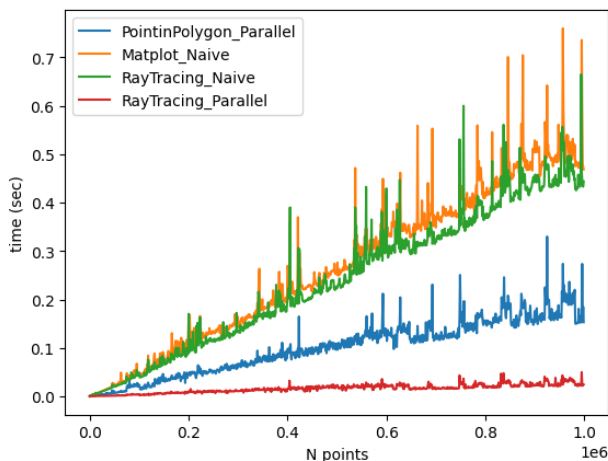


Fig. 4: Performance of various methods to employ Point-in-Polygon methods. We use the ray tracing method in our refinement layer.

V. RESULTS AND DISCUSSION

The quantitative results of our work are compared with similar methods on the Argoverse validation split dataset, as presented in Table I. To ensure fairness and consistency in the comparison, we only report the results for methods that have provided values for all $k = 1$, $k = 6$, and MR. Our main focus is on preventing off-road predictions, as evidenced by the high Driving Area Compliance (DAC) score of 0.99. This indicates that our approach effectively eliminates almost all infeasible reachable states from the prediction space used by the network. By comparing our results with the Covernet and LaneGCN, our model performed relatively well on both the minADE and minFDE aspects for $k = 6$ category, given the lower bound for our model was around 1.02. The MR of 0.22 for our *LaneGCN (Full)+Ours* was the best result when compared with the State-of-the-art, as this variant was trained from scratch without using pretrained weights for the backbone, unlike *LaneGCN (pre-trained)+Ours*. This suggests that our model trained from scratch focuses on learning more concrete representations of plausible states when presented with future reachable states and goal-oriented lanes, without compromising on the quality of the predictions.

VI. CONCLUSION AND FUTURE WORK

In this paper, we introduce a novel framework for multi-modal motion forecasting that ensures the physical feasibility of trajectories by incorporating road topology preventing off-road predictions. Our approach follows a two-step modular process. Firstly, a deterministic refinement layer is employed to generate physically reachable trajectories and goal positions. Secondly, a learnable layer captures global interactions among maps, reachable states, and feasible trajectories, providing comparative results to regression-based approaches. Going forward, we intend to explore methods to reduce the computational load of our proposed network by investigating joint trajectory forecasting involving all actors in the scene, rather than solely the target actor.

ACKNOWLEDGMENT

The research leading to these results was funded by the German Federal Ministry for Economic Affairs and Climate Action and was partially conducted in the projects “KI Wissen” and “SafeADArchitect”. Responsibility for the information and views set out in this publication lies entirely with the authors.

REFERENCES

- [1] M. Bahari *et al.*, “Vehicle trajectory prediction works, but not everywhere,” in *Proceedings of the IEEE/CVF Conference on Computer Vision and Pattern Recognition*, 2022, pp. 17 123–17 133.
- [2] M. Woon, *Physics 101: Violating universal laws*.
- [3] T. Phan-Minh *et al.*, “Covernet: Multimodal behavior prediction using trajectory sets,” in *Proceedings of the IEEE/CVF conference on computer vision and pattern recognition*, 2020, pp. 14 074–14 083.
- [4] J. Gu, C. Sun, and H. Zhao, “Densentn: End-to-end trajectory prediction from dense goal sets,” in *Proceedings of the IEEE/CVF International Conference on Computer Vision*, 2021, pp. 15 303–15 312.
- [5] M. Bansal, A. Krizhevsky, and A. Ogale, “Chauf-feurnet: Learning to drive by imitating the best and synthesizing the worst,” *preprint arXiv:1812.03079*, 2018.
- [6] P. Schörner *et al.*, “Grid-based micro traffic prediction using fully convolutional networks,” in *2019 IEEE Intelligent Transportation Systems Conference (ITSC)*, IEEE, 2019, pp. 4540–4547.
- [7] H. Cui *et al.*, “Multimodal trajectory predictions for autonomous driving using deep convolutional networks,” in *2019 International Conference on Robotics and Automation (ICRA)*, IEEE, 2019, pp. 2090–2096.
- [8] J. Gao *et al.*, “Vectornet: Encoding hd maps and agent dynamics from vectorized representation,” in *Proceedings of the IEEE/CVF Conference on Computer Vision and Pattern Recognition*, 2020, pp. 11 525–11 533.
- [9] M. Liang *et al.*, “Learning lane graph representations for motion forecasting,” in *Computer Vision – ECCV 2020*, A. Vedaldi *et al.*, Eds., Cham: Springer International Publishing, 2020, pp. 541–556, ISBN: 978-3-030-58536-5.
- [10] S. Khandelwal *et al.*, “What-if motion prediction for autonomous driving,” *arXiv preprint arXiv:2008.10587*, 2020.
- [11] A. Vivekanandan, N. Maier, and J. M. Zöllner, “Plausibility verification for 3d object detectors using energy-based optimization,” in *Computer Vision – ECCV 2022 Workshops*, L. Karlinsky, T. Michaeli, and K. Nishino, Eds., Springer Nature Switzerland, 2023, pp. 602–616, ISBN: 978-3-031-25056-9.
- [12] P. Schörner, M. T. Hüneberg, and J. M. Zöllner, “Optimization of sampling-based motion planning in dynamic environments using neural networks,” in *2020 IEEE Intelligent Vehicles Symposium (IV)*, IEEE, 2020, pp. 2110–2117.
- [13] M. Vitelli *et al.*, “Safetynet: Safe planning for real-world self-driving vehicles using machine-learned policies,” in *2022 International Conference on Robotics and Automation (ICRA)*, 2022, pp. 897–904.
- [14] M. Zhu *et al.*, “Safe, efficient, and comfortable velocity control based on reinforcement learning for autonomous driving,” *Transportation Research Part C: Emerging Technologies*, vol. 117, p. 102 662, 2020.
- [15] H. Cui *et al.*, “Deep kinematic models for kinematically feasible vehicle trajectory predictions,” in *2020 IEEE International Conference on Robotics and Automation (ICRA)*, 2020, pp. 10 563–10 569.
- [16] H. Girase *et al.*, “Physically feasible vehicle trajectory prediction,” *arXiv preprint arXiv:2104.14679*, 2021.
- [17] H. Song *et al.*, “Learning to predict vehicle trajectories with model-based planning,” in *Conference on Robot Learning*, PMLR, 2022, pp. 1035–1045.
- [18] M.-F. Chang *et al.*, “Argoverse: 3d tracking and forecasting with rich maps,” in *Proceedings of the IEEE/CVF conference on computer vision and pattern recognition*, 2019, pp. 8748–8757.
- [19] A. Vaswani *et al.*, “Attention is all you need,” in *Advances in Neural Information Processing Systems*, I. Guyon *et al.*, Eds., vol. 30, Curran Associates, Inc., 2017.
- [20] K. He *et al.*, “Deep residual learning for image recognition,” in *Proceedings of the IEEE conference on computer vision and pattern recognition*, 2016, pp. 770–778.
- [21] H. Zhao *et al.*, “Tnt: Target-driven trajectory prediction,” in *Conference on Robot Learning*, PMLR, 2021, pp. 895–904.
- [22] D. P. Kingma and J. Ba, “Adam: A method for stochastic optimization,” in *3rd International Conference on Learning Representations, ICLR 2015, San Diego, CA, USA, May 7-9, 2015, Conference Track Proceedings*, Y. Bengio and Y. LeCun, Eds., 2015.